Development status of efficiency improvement at the Rare-RI Ring facility*

Y. Yamaguchi[1†] A. Yano[1,2] T. Ohnishi[1] Y. Abe[1] N. Chandrakumar[1,3] G. Hudson-Chang[1,3] N. Imai[4] Y. Kikuchi[5] N. Kitamura[4] R. Kojima[4] J. Li[1,4] T. Moriguchi[2] D. Nagae[6] S. Naimi[7] S. Nishizawa[5] A. Ozawa[2] F. Suzaki[8] K. Takiura[5] N. Tomioka[5] R. Tuchiya[9] M. Wakasugi[10] K. Watanabe[5] T. Yamaguchi[5,11] R. Yokoyama[4] H. Zhang[2]

[1]RIKEN Nishina Center, Wako, 351-0198, Japan
[2]Institute of Physics, University of Tsukuba, Tsukuba, 305-8571, Japan
[3]Department of Physics, University of Surrey, Guildford, GU2 7XH, UK
[4]Center for Nuclear Study, University of Tokyo, Wako, 351-0198, Japan
[5]Graduate School of Science and Engineering, Saitama University, Saitama, 338-8570, Japan
[6]Laboratory for Zero-Carbon Energy, Tokyo Institute of Technology, Tokyo 152-8550, Japan
[7]Paris-Saclay University, CNRS/IN2P3, IJCLab, Orsay, 91405, France
[8]Advanced Science Research Center, Japan Atomic Energy Agency, Ibaraki 319-1195, Japan
[9]Department of Physics, Rikkyo University, Tokyo 172-8501, Japan
[10]Institute for Chemical Research, Kyoto University, Kyoto 611-0011, Japan
[11]Tomonaga Center for the History of the Universe, University of Tsukuba, Tsukuba, 305-8571, Japan

Abstract: The rare radioactive-isotope (RI) ring is an isochronous storage ring for deriving the masses of extremely short-lived rare RIs. Since the successful commissioning experiment in 2015, the time of flight mass measurement technique has been established through test experiments using unstable nuclei with well-known masses. The experiments for unknown masses were started in 2018. While conducting experiments, we continue to develop equipment to further improve the efficiency and precision of mass measurements. The upgraded kicker system can generate a magnetic field with an extractable duration equivalent to the revolution time of the ring. This is essential for extracting extremely rare events as well as shortening the measurement time compared with that in the initial experiments. New steering magnets make it possible to eliminate an uncertain vertical beam deviation that occurs upstream. As a result, we confirm that the extraction yield is increased. A new resonant Schottky pick-up is able to detect single particles in timeframes on the order of milliseconds. It will be useful not only for beam diagnostics but also for lifetime measurement experiments of extremely short-lived rare RIs planned as a future application.

Keywords: steering magnet, kicker system, Schottky pick-up, isochronous storage ring

DOI: 10.1088/1674-1137/add25d **CSTR:** 32044.14.ChinesePhysicsC.49094002

I. INTRODUCTION

Storage rings have demonstrated their capability to expand many scientific fields, including fundamental physics, atomic and molecular physics, high energy physics, and nuclear physics. This is particularly the case in nuclear physics research using radioactive-isotope (RI) beams. Heavy-ion storage rings provide a unique opportunity for measuring the basic properties of exotic nuclei [1,2]. Focusing on mass, various excellent methods have been developed to accurately measure the mass of RI [3], but the methods are limited for extremely short-lived RIs. In this respect, isochronous mass spectrometry (IMS) is very useful. IMS using a heavy-ion storage ring was first realized by the experimental storage ring (ESR) at GSI [4,5], and this technique has been applied to the experimental cooler storage ring (CSRe) [6] at HIRFL with remarkable results in recent years [7,8].

Extending IMS to further exotic nuclei, such as those that are very neutron rich, would significantly contribute to our understanding of rapid neutron capture (*r*-process) nucleosynthesis [9], which is responsible for the production of half of the chemical elements heavier than iron in our universe [10,11]. Atomic mass is one of the basic properties for determining the *r*-process path, and mass measurements with a precision of less than 100 keV provide important data for the *r*-process modeling [12−15].

The RIKEN RI Beam Factory (RIBF) [16] is a cyclotron facility capable of producing large amounts of RI re-

Received 3 March 2025; Accepted 30 April 2025; Published online 1 May 2025

* Supported by RIKEN Pioneering Project funding and JSPS KAKENHI (17H01123, 18H03695, 21H04461, 23K25876.)

† E-mail: yamaguch@ribf.riken.jp

lated to the *r*-process. In fact, important results that have advanced our understanding of the *r*-process have been achieved so far by measuring the half-lives of neutron-rich nuclei [17, 18] and their neutron emission probabilities [19]. Because it was clear that mass measurement also plays an important role in making the best use of the RIBF, it was necessary to construct a heavy-ion storage ring dedicated to the IMS method. However, the combination of a cyclotron and storage ring is incompatible, because a storage ring requires a pulsed operation, whereas a cyclotron delivers a continuous beam. We accordingly solved this incompatibility by synchronizing the injection with the particle production timing and eventually constructed the Rare-RI Ring (R3) [20, 21].

II. RARE-RI RING FACILITY

The primary beam supplied by the superconducting ring cyclotron (SRC) [22] is sent to the F0 production target of the in-flight fragment separator BigRIPS [23] to produce various RI beams. The particle selection and identification can be performed at BigRIPS on an event-by-event basis [24]. R3 connects to the BigRIPS via the OEDO-SHARAQ system [25], as shown in Fig. 1. The trigger signal that activates the R3 fast-response kicker system [26] originates from a signal generated when a particle passes through the F3 timing detector. This signal is processed as a logic signal by the dedicated modules [27] and then immediately transmitted to the kicker system by an air-gapped coaxial copper tube. The trigger signal excites the kicker magnetic field in synchronization with the particle's arrival at the kicker magnet. The concept of this method was proposed by I. Meshkov *et al.* [28] as an individual injection, and it was first realized at R3.

R3 is a six-fold symmetrical storage ring with a circumference of approximately 60 m, and twenty-four bending magnets form its lattice structure. The bending magnets are reused from TARN-II [29]. The isochronous condition can be precisely adjusted over a wide momentum range using trim-coils [30]. The trim-coils are equipped on the outer two bending magnets of each four-magnet sector. The best case so far for the isochronous condition ($\delta T/T$) is 2.8 ppm over a momentum spread (dp/p) of approximately 0.45% [31]. The dispersion and emittance matching at the center of the kicker system is important to keep the injection efficiency. An in-ring detector, the E-MCP [32], is used to confirm that the particles are circulating properly after injection. Once confirmed, the E-MCP will be evacuated from the equilibrium orbits. After circulation of a minimum of 0.7 ms, the particles are kicked again by the same kicker magnet and extracted from the extraction septum. The R3 facility, which performs a sequence of operation, injection, circulation, and extraction at up to 100 Hz, is a unique storage ring facility capable of handling single particles.

The time of flight (ToF) is measured between the BE-MCP [33, 34] located at the S0 focal plane for the start signal and a plastic scintillator located at the extraction beam-line (ELC) from R3 for stop. The revolution time ($T_{\rm rev}$) of a particle is derived by dividing the measured ToF by the number of turns. The number of turns is determined as an integer using the periodic signal information of the E-MCP. Precision of the periodic signal is on the order of 10^{-4}, thereby making it possible to distinguish a difference of one turn over several thousand turns. The unknown mass (m_1) of a nucleus is determined relative to the well-known mass (m_0) of a reference nucleus. Assuming perfect isochronous condition holds for the reference nucleus, its revolution time T_0 is constant regardless of the momentum. In this case, however, because the other nuclei are non-isochronous, their revolution time T_1 must be corrected by using their velocity or magnetic rigidity. The currently used technique is well described in [35], and the first results can be found in [36].

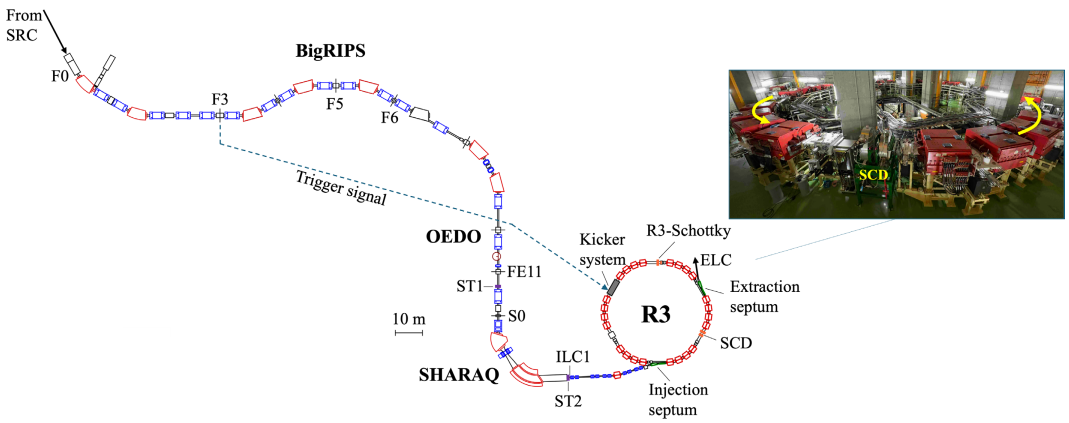

Fig. 1. (color online) The R3 connects to the BigRIPS via the OEDO-SHARAQ system. The trigger signal for activating the R3 kicker system is generated at the F3 focal plane of the BigRIPS.

III. DEVELOPMENTS FOR EFFICIENCY IMPROVEMENT

There are two key factors for precisely measuring the masses of the most exotic nuclei produced at the BigRIPS. One is to increase the transmission efficiency from BigRIPS-F3 to R3-ELC. The vertical deviation of the beam that occurs upstream of the BigRIPS is one of the main causes of beam loss. If the vertical aperture is wide enough, there is no effect of this deviation. However, downstream from the ILC1 focal plane (see Fig. 1), the vertical aperture is quite narrow, less than one-third the size of the upstream one, and it is difficult to reduce the optical magnification, thereby resulting in significant beam loss. In addition, there is no vertical steering magnet in the BigRIPS. To solve this beam loss problem, we have installed vertical steering magnets dedicated to the R3.

Another key factor is to improve the ToF measurement efficiency. The ToF for several nuclides is measured through the extraction process. However, after several thousand turns, each nuclide is distributed at a different position inside the ring, owing to the different velocities. Because the extractable duration of the kicker system is shorter than the revolution time, it becomes impossible to extract each nuclide using the same timing, and it is time-consuming to extract all nuclides. We have, therefore, upgraded the kicker system to lengthen the extractable magnetic field flat-top.

A. Steering magnets installation

Two steering magnets were installed without changing the existing magnets arrangement in the beam-line. One (ST1) is in the straight section after FE11 focal plane of the OEDO-SHARAQ system and the other (ST2) is just before ILC1. By installing steering magnets in such locations, it was simulated that any upstream vertical deviations experienced so far can be handled with a deflection angle of a few mrad, i.e., the transmission efficiency can be restored to almost the same as that without the upstream deviations. The overall design and optimum magnetic pole geometry were studied and fabricated to be as compact as possible. Magnetic field measurements were then performed to confirm that the magnetic field distribution is obtained as designed. Table 1 summarizes the specifications of steering magnets when a beam with the magnetic rigidity of 6.4 Tm needs to be deflected by 2 mrad as an example. The indirect water-cooling method was adopted, and the amount of water flow required to keep the average temperature rise of the entire coil within 20℃ is 2 ℓ/min.

Recently, a test experiment of the steering magnets with a ^{124}Xe beam, which has magnetic rigidity of approximately 4.3 Tm, was performed. The vertical deviations measured at BigRIPS-F3 were $y_{f3} \approx -2$ mm and $y'_{f3} \approx -2.7$ mrad for the position and angle of the center of beam distribution, respectively. Two position detector PPACs [37] were installed in the kicker chamber. Figure 2 shows the current dependence of the steering magnets on the vertical position y_{kc} and angle y'_{kc} of the center of beam distribution at the kicker center. Both y_{kc} and y'_{kc} are strongly dependent on the current of ST1 in this case, which is consistent with the simulation result. It can also be seen that, when the currents of ST1 and ST2 are -7 A and 7 A, y_{kc} and y'_{kc} are appropriately corrected. In this test experiment, when the steering magnets were used at the optimum currents shown in Fig. 2, the extraction yield was more than 7 times higher than when the steering magnets were not used. Details of the design study, fabrication, and results of the test experiment will be described elsewhere.

Table 1. Specifications of the steering magnets

	ST1	ST2
Pole length [m]	0.3	0.25
Pole gap [m]	0.17	0.125
Flux density [T]	0.043	0.051
Turn number [T/P]	204	204
Current [A]	15.0	13.1
Weight [kg]	180	110

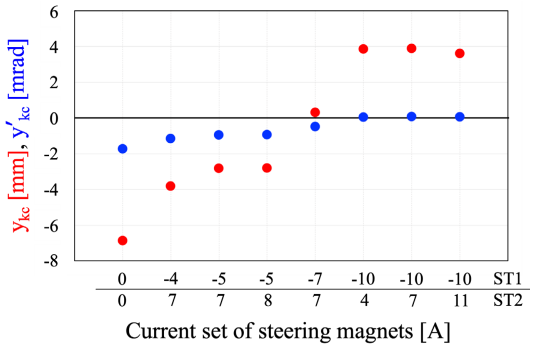

Fig. 2. (color online) Red and blue circles show the center of beam distribution for the vertical position y_{kc} and angle y'_{kc} at the kicker center, respectively. The horizontal axis indicates the combination of the currents of the two steering magnets.

B. Kicker system upgrade

The kicker system is particularly important for the R3 facility. The conditions are unique, not only requiring a fast response to establish the individual injection method but also ensuring that the injected particles are not affected by any magnetic fields when they pass through the kicker magnet again. A wide horizontal aperture is essential for the dispersion and emittance matching during injection, therefore a distributed constant twin-type kicker is adopted. Impedance matching is considered by taking

into account the effect of mutual inductance of twin-type kicker facing each other to obtain a magnetic field that satisfies the above conditions. The obtained magnetic field waveform is shaped like a half-sinusoidal wave, with the rise and fall times, and duration of around 100 ns [38]. The duration of 100 ns is sufficient for the injection process. In contrast, it is not sufficient for the extraction process, because the typical revolution time of a circulated particle is approximately 385 ns at an energy of 160 MeV/u.

We created two different magnetic field distributions by changing the impedance matching condition so that the magnetic field for the particles would meet our requirements. This was because a new pulsed power supply would be needed to create the required shape of magnetic field distribution from scratch, as briefly mentioned in the final section. The upper part of Fig. 3 shows the layout of the twin-type kicker magnets; the middle and lower parts show the magnetic field distributions for injection and extraction, respectively. Following excitation

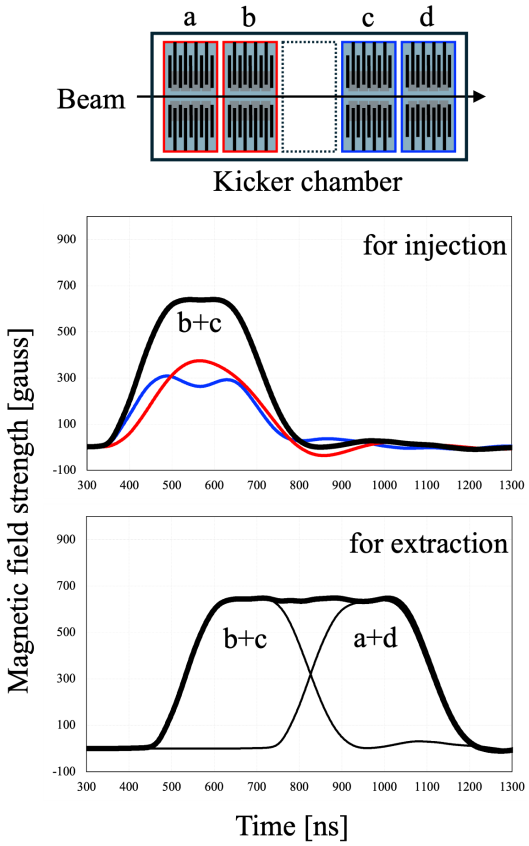

Fig. 3. (color online) Layout of the four twin-type kicker magnets inside the chamber. Center and lower panels show the magnetic field distributions for injection and extraction, respectively. For injection, red and blue lines indicate the measured magnetic fields by a one-turn search coil at a charging voltage of 25 kV. Thick-solid lines show the total magnetic fields by each unit.

for injection, the same kicker magnet can be excited for extraction after a duration as short as 0.7 ms. Two magnets are used for injection and all four are used for extraction. When a particle passes through units b and c, it experiences two different magnetic field distributions. If the timing is precisely tuned, all particles can be injected at the flat-top region, indicated by the thick-solid line in the center panel of Fig. 3. For extraction, units b and c are re-excited first, followed by units a and d a few hundred nanoseconds later. This sequential approach leads to an extended flat-top duration, as illustrated by the thick-solid line in the lower panel of Fig. 3. The extended flat-top duration of approximately 400 ns covers the typical revolution time, thereby ensuring that circulating particles can always be extracted.

This approach worked well in previous experiments. We succeeded in extracting all five nuclides, which were injected into R3, with a single extraction time setting by using a sufficiently long magnetic field distribution, as described in [31]. However, owing to the high charging voltage, breakdown of the insulation of the ceramic charging capacitors in the pulsed power supplies occurred frequently. The capacitors used so far were three-layer capacitors (HP40-H132-00) insulated with molded resin. As a result of a failure analysis, the central part of the three-layer structure was found to be particularly damaged. We were not able to pinpoint the cause. It was thought that the stacked elements structure could not withstand the constant use of high repetition (200 μs), high voltage charging and instantaneous discharging by a thyratron. We ultimately decided to replace the capacitors with single-layer capacitors (FHV-10AN). After that, a long-term operation test was conducted with all four units, which demonstrated that they could operate without any problems for several days even under the condition that previously caused failures [39]. Mass measurements of rare-RIs, whose extraction timing cannot be identified in advance, will become possible in the near future experiments.

IV. NEW RESONANT SCHOTTKY PICK-UP

A beam diagnostics device capable of non-destructively measuring the revolution frequency of charged particles is indispensable for the storage ring. A highly sensitive resonant Schottky pick-up was developed at ESR [40] and another has been installed in CSRe [41]. A similar one is also installed in R3, consisting of a pillbox-type cavity and a beam duct with ceramic gap [42]. The aim with R3 is to adjust the isochronous conditions using a single ion, which has been successfully demonstrated in previous experiments [43]. Development of resonant Schottky pick-ups is ongoing, and the latest version [44] installed in ESR has been successfully utilized for the decay study experiments [45].

Recently, we have developed a new type of resonant Schottky pick-up. The concepts are as follows: extension of the frequency band adjustment range, miniaturization, cost reduction, and sensitivity improvement, compared with the original one. A detailed design study was carried out using simulation software CST . By providing two tuners, one large and one small, the frequency band adjustment range is 5.35 MHz, which covers one harmonic range of R3 (around 3 MHz). A tuning accuracy of 1 kHz can be achieved. A rectangular shape is adopted so that it can be installed inside the existing vacuum chamber of R3. Hence, a ceramic gap is not required and high sensitivity can be achieved at a low cost. The use of oxygen-free copper, which has excellent electrical conductivity, as the cavity material also contributes to improving the cavity sensitivity. Figure 4 is a photograph of the rectangular-type cavity fabricated in this study. It is fixed to the chamber lid so that it hangs from the lid when installed inside the chamber. The quality factor was measured using a vector network analyzer after the coupler geometry was adjusted to achieve characteristic impedance matching between the cavity and the external circuits. The shunt impedance was evaluated by the bead-pull measurement method in air. Table 2 shows the measurements compared with those of the original one. Figure 5 shows an example of time versus frequency spectrogram of single particle obtained with $^{124}Xe^{54+}$ beam at an energy of approximately 155 MeV/nucleon. The frequency span was 1 MHz. The frame length was set to approximately 2.2 ms in this example. The measurement sequence was set to 100 Hz injection only. It can be consequently interpreted that particle-a was injected with an injection kick and completely disappeared with the next injection kick after 10 ms of circulation, whereas particle-b was successfully injected on the same kick. The resonance frequencies for particles-a and -b were 503.59015 MHz and 503.57347 MHz, respectively. Because the isochronous condition was not adjusted precisely at this measurement, the two particles with different momenta showed different frequencies on the order of 10^{-5}. This new resonant Schottky pick-up will be useful for lifetime measurement experiments of extremely short-lived rare RIs, including the isomeric states.

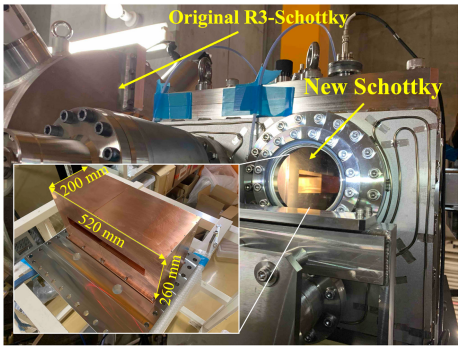

Fig. 4. (color online) New resonant Schottky pick-up, which has a rectangular shape, is installed in the existing vacuum chamber. The original pillbox-type R3-Schottky is located next to the new one.

Table 2. Characteristic comparison.

	New	Original
Resonance frequency f_0/MHz	503	171
Shunt impedance R_{sh}/kΩ	3000	160
Unloaded quality factor Q_0	14000	1880
Loaded quality factor Q_L	7000	1250
(R_{sh}/Q_0)/Ω	210	85

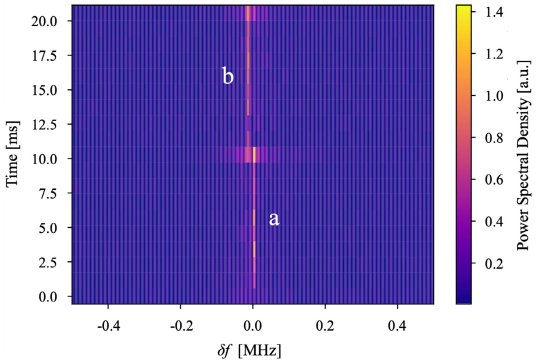

Fig. 5. (color online) Time versus frequency spectrogram of single particle detection for $^{124}Xe^{54+}$. See the text for details.

V. SUMMARY AND OUTLOOK

By installing two vertical steering magnets dedicated to R3 in the appropriate locations, the extraction yield was successfully increased. The results of the test experiment using a ^{124}Xe beam showed that adjusting the vertical position at the kicker center is important for increasing the extraction yield. In upcoming experiments using four twin-type kicker magnets, one PPAC will be installed at the center of the kicker chamber to adjust the steering magnets while checking the vertical position information. Alternatively, we may use the DL-E-MCP [46], which can measure the position of a circulating particle using the combination of a conversion foil and a delay-line MCP. It will be installed in the straight section after the kicker chamber. The conversion foil that a particle passes through for each revolution is sufficiently thin to make several dozen revolutions. Therefore, we expect that this detector can also be used to measure ring parameters such as the betatron tune.

A sufficiently long kicker magnet extraction field was achieved by properly adjusting the magnetic field waveforms and excitation timing of the four twin-type kicker magnets. Furthermore, stable operation of the pulsed power supplies of the kicker magnets was realized by

changing the ceramic capacitors for the entire charging system. As a result, mass measurement experiments can be resumed. Meanwhile, further upgrades to the pulsed power supply are also being considered. This is a change from the thyratron switch method to a semiconductor switch method using a linear transformer driver circuit [47]. The advantages are numerous: the injection repetition frequency can be dramatically increased up to 100 times (10 kHz), and the response becomes faster; hence, the injection beam energy can be increased, and a very short pulse magnetic field can be created and adjusted on the order of nanoseconds. There are two main reasons for this change. One is that it is better to inject/extract at the same angle as much as possible for all nuclides. Recent data analysis and simulations have revealed that this fact is important for more precise mass determination. The other is that we have a plan to operate the R3 as an isomer filtering device. A feasibility study showed that the semiconductor switch method is essential for this purpose [48].

In addition to the rectangular-type cavity, which was successfully demonstrated with ^{124}Xe beam, a position-sensitive resonant Schottky pick-up was installed in a straight section of R3. The conceptual design using an elliptical cavity has been discussed about a decade ago [49]. This Schottky cavity doublet (SCD) was designed specifically for R3 [50]. Replacing the currently used flight-time measurement technique with measurements only inside the ring using the SCD is expected to improve the accuracy of mass determination and the transmission efficiency of nuclei, especially in the high-Z region. A pilot experiment will be conducted soon. The detector's details can be found in [51–52].

ACKNOWLEDGMENTS

Beam commissioning was performed at the RIBF operated by the RIKEN Nishina Center and the CNS, University of Tokyo.

References

[1] Y. H. Zhang, Yu. A. Litvinov, T. Uesaka *et al.*, Phys. Scripta **91**, 073002 (2016)
[2] M. Steck and Yu. A. Litvinov, Prog. Part. Nucl. Phys **115**, 103811 (2020)
[3] T. Yamaguchi, H. Koura, Yu. A. Litvinov, Prog. Part. Nucl. Phys. **120**, 103882 (2021)
[4] B. Franzke, Nucl. Instrum. Methods Phys. Res., Sect. B **24/25**, 18 (1987)
[5] M. Hausmann, F. Attallah, K. Beckert *et al.*, Nucl. Instrum. Methods Phys. Res., Sect. A **446**, 569 (2000)
[6] J. W. Xia, W. L. Zhan, B. W. Wei *et al.*, Nucl. Instrum. Methods Phys. Res., Sect. A **488**, 11 (2002)
[7] X. Zhou, M. Wang, Y. H. Zhang *et al.*, Nat. Phys. **19**, 1091 (2023)
[8] M. Wang, Y. H. Zhang, X. Zhou *et al.*, Phys. Rev. Lett. **130**, 192501 (2023)
[9] E. Burbidge, G. R. Burbidge, W. A. Fowler *et al.*, Rev. Mod. Phys. **29**, 547 (1957)
[10] J. J. Cowan, C. Sneden, J. E. Lawler *et al.*, Rev. Mod. Phys. **93**, 015002 (2021)
[11] T. Kajino, W. Aoki, A. B. Balantekin *et al.*, Prog. Part. Nucl. Phys. **107**, 109 (2019)
[12] D. Martin, A. Arcones, W. Nazarewicz *et al.*, Phys. Rev. Lett. **116**, 121101 (2016)
[13] Y. Motizuki, T. Tachibana, S. Goriely *et al.*, The Future Astronuclear Phys. **11**, 227 (2004)
[14] M. Mumpower, R. Surman, D. L. Fang *et al.*, J. Phys. G: Nucl. Phys. **42**, 034027 (2015)
[15] R. Utama and J. Piekarewicz, Phys. Rev. C **97**, 014306 (2018)
[16] Y. Yano, Nucl. Instrum. Methods Phys. Res., Sect. B **261**, 1009 (2007)
[17] G. Lorusso, S. Nishimura, Z. Y. Xu *et al.*, Phys. Rev. Lett. **114**, 192501 (2015)
[18] J. Wu, S. Nishimura, G. Lorusso *et al.*, Phys. Rev. Lett. **118**, 072701 (2017)
[19] V. H. Phong, S. Nishimura, G. Lorusso *et al.*, Phys. Rev. Lett. **129**, 172701 (2022)
[20] A. Ozawa *et al.* (Rare-RI Ring collaboration), Prog. Theor. Exp. Phys. **2012**, 03C009 (2012)
[21] Y. Yamaguchi, M. Wakasugi, T. Uesaka *et al.*, Nucl. Instrum. Methods Phys. Res., Sect. B **317**, 629 (2013)
[22] H. Okuno, K. Yamada, J. Ohnishi *et al.*, IEEE Trans. Appl. Supercond. **17**, 1063 (2007)
[23] T. Kubo, D. Kameda, H. Suzuki *et al.*, Prog. Theor. Exp. Phys. **2012**, 03C003 (2012)
[24] N. Fukuda, T. Kubo, T. Ohnishi *et al.*, Nucl. Instrum. Methods Phys. Res., Sect. B **317**, 323 (2013)
[25] M. Michimasa, T. Chillery, J. W. Hwang *et al.*, Nucl. Instrum. Methods Phys. Res., Sect. B **540**, 194 (2023)
[26] Y. Yamaguchi, H. Miura, M. Wakasugi *et al.*, Phys. Scr. **T166**, 014056 (2015)
[27] Y. Abe, Y. Yamaguchi, M. Wakasugi, *et al.*, RIKEN Accel. Prog. Rep. **52**, 15 (2019)
[28] I. Meshkov, W. Mittig, P. Roussel-Chomaz *et al.*, Nucl. Instrum. Methods Phys. Res., Sect. A **523**, 262 (2004)
[29] T. Katayama, K. Chiba, T. Honma *et al.*, Part. Accel. **32**, 105 (1990)
[30] Y. Abe, Y. Yamaguchi, M. Wakasugi *et al.*, Nucl. Instrum. Methods Phys. Res., Sect. A **1072**, 170083 (2025)
[31] S. Naimi, Y. Yamaguchi, T. Yamaguchi *et al.*, Eur. Phys. J. A, **59**, 90 (2023)
[32] D. Nagae, Y. Abe, S. Okada *et al.*, Nucl. Instrum. Methods Phys. Res., Sect. A **986**, 164713 (2021)
[33] S. Suzuki, A. Ozawa, D. Kamioka *et al.*, Nucl. Instrum. Methods Phys. Res., Sect. A **965**, 163807 (2020)
[34] T. Moriguchi, M. Mukai, N. Kaname *et al., Improvements of time-of-flight detector utilizing a thin foil and crossed static electric and magnetic fields* Chin. Phys. C, to be published.
[35] D. Nagae, S. Omika, Y. Abe *et al.*, Phys. Rev. C **110**, 014310 (2024)

[36] H. F. Li, S. Naimi, T. M. Sprouse *et al*., Phys. Rev. Lett. **128**, 152701 (2022)
[37] H. Kumagai, T. Ohnishi, N. Fukuda *et al*., Nucl. Instrum. Methods Phys. Res., Sect. B **317**, 717 (2013)
[38] H. Miura, Y. Abe, Z. Ge, *et al*., in Proceedings of HIAT2015, MOPA23 (2015).
[39] Y. Yamaguchi, A. Yano, T. Ohnishi, *et al*., RIKEN Accel. Prog. Rep. **57**, 109 (2024)
[40] F. Nolden, P. Hülsmann, Yu. A. Litvinov *et al*., Nucl. Instrum. Methods Phys. Res., Sect. A **659**, 69 (2011)
[41] J. X. Wu, Y. D. Zang, F. Nolden *et al*., Nucl. Instrum. Methods Phys. Res., Sect. B **317**, 623 (2013)
[42] F. Suzaki, Y. Abe, A. Ozawa *et al*., Phys. Scr. **T166**, 014059 (2015)
[43] F. Suzaki, Y. Abe, M. Wakasugi, *et al*., RIKEN Accel. Prog. Rep. **59**, 52 (2019)
[44] M. S. Sanjari, D. Dmytriiev, Yu. A. Litvinov *et al*., Rev. Sci. Instrum. **91**, 083303 (2020)
[45] D. Freire-Fernández, W. Korten, R. J. Chen *et al*., Phys. Rev. Lett. **133**, 022502 (2024)
[46] G. Hudson-Chang, S. Naimi, Y. Abe *et al*., Nucl. Instrum. Methods Phys. Res., Sect. A **1069**, 169980 (2024)
[47] W. Jiang, H. Sugiyama, and A. Tokuchi, IEEE Trans. Plasma Sci. **42**, 11 (2014)
[48] Y. Yamaguchi, T. Ohnishi, and T. Yamaguchi, RIKEN Accel. Prog. Rep. **57**, 108 (2024)
[49] M. S. Sanjari, X. Chen, P. Hülsmann, *et al*., Phys. Scr. **T166**, 014060 (2015)
[50] D. Dmytriiev, *Design of a Position Sensitive Resonant Schottky Detector for the Rare-RI Ring in RIKEN*, Ph.D. Thesis (Heidelberg: University of Heidelberg, 2022).
[51] G. Hudson-Chang, S. Sanjari, S. Naimi *et al*., *A minimisation method for accurate position-determination using a position-sensitive Schottky cavity doublet* Chin. Phys. C, to be published
[52] S. Sanjari, Y. A. Litvinov, G. Hudson-Chang *et al*., *Schottky detection techniques for ultra-rare short-lived ions in heavy ion storage rings* Chin. Phys. C, to be published